5-2021

Aloe Vera extract-based composite nanofibers for wound dressing applications

Raul Barbosa

Alexa Villarreal

Cristobal Rodriguez

Heriberto De Leon

Robert Gilkerson

See next page for additional authors

Authors

Raul Barbosa, Alexa Villarreal, Cristobal Rodriguez, Heriberto De Leon, Robert Gilkerson, and Karen Lozano

Version of Record: https://www.sciencedirect.com/science/article/pii/S0928493121002009
Manuscript_fb5fdd8981ca9f3c6b3fafe244097235

Aloe Vera Extract-Based Composite Nanofibers For Wound Dressing Applications

Raul Barbosa,[1] Alexa Villarreal,[1] Cristobal Rodriguez,[2] Heriberto De Leon,[1] Robert Gilkerson,[2] and Karen Lozano*[1]

[1]Department of Mechanical Engineering, University of Texas Rio Grande Valley, Edinburg, TX 78539, USA

[2]Department of Biology, University of Texas Rio Grande Valley, Edinburg, TX 78539, USA

*To whom correspondence should be addressed: karen.lozano@utrgv.edu, +1-956-665-7020.

Abstract

Natural, biocompatible, and biodegradable composite nanofibers made of Aloe vera extract, pullulan, chitosan, and citric acid were successfully produced via Forcespinning® technology. The addition of Aloe vera extract at different weight percent loadings was investigated. The morphology, thermal properties, physical properties, and water absorption of the nanofibers were characterized using scanning electron microscopy (SEM), Fourier transform infrared spectroscopy (FTIR), and thermogravimetric analysis (TGA). The developed nanofiber membranes exhibited good water absorption capabilities, synergistic antibacterial activity against Escherichia coli, and promoted cell attachment and growth. Its porous and high surface area structure make it a potential candidate for wound dressing applications due to its ability to absorb excessive blood and exudates, as well as provide protection from infection while maintaining good thermal stability.

Keywords: Aloe vera, biomaterials, Forcespinning®, wound dressing, composite nanofibers, pullulan

1. Introduction

Wound healing is a normal biological response in the human body achieved through four sequential phases: hemostasis, inflammation, proliferation, and remodeling [1]. Effective and efficient wound healing is possible through harmonious and timely achievement of the aforementioned phases. However, there are several factors such as infection, poor blood supply, presence of necrotic tissue, inadequate nutrition, and advanced age that can adversely affect this process which may lead to chronic wounds and improper tissue repair [2]. This results in a delayed or incomplete healing process which can cause significant burden to the patients, healthcare system, and society [3].

Novel wound dressings, such as nanofibers (NFs), have been designed to treat and enhance the natural restorative response of the healing process. The study of NF-based membranes for wound dressings and scaffolds has increased in recent years due to its high surface area, nano porosity, and the ability to incorporate biomolecules or medications [4]. The use of biomaterials in the fabrication of the aforementioned membranes can provide additional properties such as biocompatibility, biodegradability, antibacterial activity, and adequate mechanical stability.

Aloe vera and pullulan are biomaterials that provide ideal features and advantages for wound management aid. Aloe (also known as *Aloe vera* (L.) Burm.f.) is a type of succulent plant that belongs to the *Aloaceae* family [5]. It has been used medicinally for centuries in numerous cultures for a variety of purposes due to its healing properties. It contains more than 75 potentially active constituents including minerals, vitamins, amino acids, saccharides, enzymes, lignin, anthraquinones, salicylic acids, and saponins. There are a number of studies trying to identify and evaluate which of these substances are responsible for its healing effects. However, some research

suggests that the synergistic interaction between the compounds, rather than a single component, is responsible for the plant's beneficial properties [6]. For example, numerous reports investigating the benefits of *A. vera* have shown positive results in burn-wound treatments [7, 8]; wound healing [9, 10]; scaffolds [11, 12]; and antibacterial [13], antiviral [14], and immunostimulative activity [15], among other health advantages.

Pullulan is an extracellular and neutral microbial polysaccharide produced by the fungus *Aureobasidium pullulans* in sugar and starch cultures [16]. It consists of a linear structure with maltotriose units connected by a (a)-1,6 glycosidic bond. Due to its structure, pullulan is flexible, exhibits a high solubility in water while being insoluble in organic solvents, and is non-hygroscopic. Furthermore, pullulan is biodegradable, nontoxic, noncarcinogenic, nonmutagenic, and edible [17]. It also shows good mechanical strength, decomposes at temperatures of 250-280 ºC, and can be used to form thin layers, nanoparticles, NFs, and flexible coatings [17]. Pullulan's remarkable properties make it an important source of polymeric materials, which can be utilized in a wide range of applications. Its commercial production began in 1976 in Japan and is currently used in industrial applications such as a blood plasma substitute, food additive, a film, and as an adhesive [18]. Pullulan is used extensively for biomedical purposes due to its inert nature, biocompatibility, low oxygen permeability, and chemical and mechanical properties. Examples include targeted drug and gene delivery [19], medical imaging [20], vaccination [21], and wound healing [22].

The usage of pullulan for wound healing applications has generated positive results by a number of different investigations. Li *et al*. [23] synthesized a hydrogel made of a pullulan derivative and cystamine with antimicrobial agents resulting in good swelling capacity, high water absorption, great mechanical strength, effective antimicrobial release activity, and

biocompatibility. These results support pullulan for use in wound dressings for clinical applications. Hydrogels can also be modified to form synthetic dermal scaffolds that serve as structural templates for wound repair. For example, Wong *et al.* [22] fabricated a pullulan-collagen scaffold using a salt-induced phase inversion technique which resulted in an augmented early wound healing. Pullulan NF membranes also hold great potential for skin tissue engineering. Xu *et al*. [24] developed a ternary nanofibrous membrane composed of pullulan, chitosan, and tannic acid that showed non-cytotoxicity, antibacterial properties, enhanced cell proliferation and attachment, good water stability and absorption.

In this study, composite NF-based membranes containing *A. vera* extract, pullulan, chitosan and citric acid were developed via Forcespinning® for wound dressing applications. Forcespinning® is a process that employs centrifugal forces to produce superfine fibers with sizes ranging from micro to nanometer [25]. This method does not depend on electrostatic charges and/or sample conductivity thus a broader number of new materials (both solution and polymer melt) could be spun into nanofibers [26]. In addition, Forcespinning® provides a higher nanofiber yield and ease of production compared to electrospinning, which allows for large scale fiber production [27]. The morphology, water absorption, and thermal properties of the produced NFs were investigated. Their biocompatibility was evaluated in vitro with mouse embryonic fibroblast cells (NIH 3T3), and the antibacterial activity was tested against gram-negative bacteria, *Escherichia coli*.

2. Materials and Methods

2.1 Materials

Pullulan (PL) was purchased from Tokyo Chemical Industry Co. (Japan). Chitosan (CH) with a low–molecular weight (MW = 50,000–190,000 and 75%–85% degree of deacetylation) was purchased from Sigma–Aldrich (St Louis, USA). Citric Acid (CA) was purchased from Sigma–Aldrich (St Louis, USA). *A. vera* leaf extract was filtered and used without further treatment. Deionized (DI) water was produced from a Smart2Pure water purification system. 30-gauge with an inner diameter of 0.159 mm bevel needles (PrecisionGlide™) were purchased from Fisher scientific for the use of fiber production process. Dulbecco's Modified Eagle Medium (DMEM (1X)) (Gibco™) was purchased from Thermo Fisher Scientific, and phosphate buffered saline (10X PBS solution) from Fisher-Bioreagents™.

2.2 Aloe Vera Extract Preparation

An *A. vera* leaf was washed with DI water and dried at ambient temperature. The leaf was cut from both ends and left to drain excess liquid. The bottom flat side of the leaf was skinned and was once again rinsed with DI water to ensure a clean specimen. A sanitized spatula was used to scrape off the *A. vera* extract (AVE) which was then placed in a glass container. The collected extract was filtered using a 50 µm syringe filter. The filtered AVE was collected into a separate glass container and stored in a fridge at 15 °C for further experimental use.

2.3 Solution Preparation

For the control solution (control), 10 mL of DI water was placed in a 20 mL vial and mixed with 400 mg of CA until completely dissolved. Then, 500 mg of CH were added to the aqueous solution and vortexed until homogeneity was achieved. The CA/CH solution was left to stir over

night using a magnetic stirring rod. Later, 2 grams of PL were added to the CA/CH solution, homogenized, and left to stir for a minimum of 6 hours.

For the remaining solutions, different AVE/DI water concentrations were prepared in order to observe the influence of the AVE concentration on the fiber diameter, thermal stability, antibacterial effect, and cell growth proliferation. The AVE/DI water ratios (v/v) consisted of 2/8, 6/4, and 10/0 mL per solution and were designated as 20%, 60%, and 100% extract, respectively. The same concentrations of CA, CH, and PL were added following the same procedures used for the control sample.

2.4 Fiber membrane development

Fibers were developed using the Forcespinning® process which uses centrifugal forces to create NFs in a controlled chamber with adjustable parameters such as angular velocity and time. To produce the fibers, a 3 mL syringe was used to inject 2 mL of the prepared solution in a spinneret of the Cyclone™ L-1000M, purchased from FibeRio Technology Corporation (McAllen, USA). The prepared solution was spun at angular velocities ranging from 4000 to 7000 RPM at 19 ºC with 45%-55% humidity. The solution was ejected from both ends of the spinneret through the 30-gauge needles, and was deposited onto equally distanced vertical pillars. Fibers were then manually collected using a 10 cm x 10 cm hollow frame after each cycle. Layers of NF were laid on top of one another as these were collected. Collected nonwoven membranes were then covered and stored in a low moisture environment as shown in previous reports [28].

2.5 Cross-linking

Once the spinning process was completed, the collected composite NF membranes were placed in an oven at 140 °C in an air atmosphere for 1 hour to allow the CA to properly cross-

linking the system. The cross-linking process allows the composite NFs to become insoluble in water. The sample was then taken out of the oven and left to dry for further analysis.

2.6 NFs Characterization

A scanning electron microscope (Zeiss EVO LS10) was used to analyze the morphology and average diameter of the fibers. The magnifications range from 300X to 1500X and a voltage of 1-3kV was used throughout the process. The NFs average diameter was calculated by indiscriminately measuring the diameter of 100 different NFs from SEM images using the image analysis software ImageJ.

Thermogravimetric analysis (TGA) was completed using a Netzsch TG 209 at a rate of 10 °C/min with temperatures increasing from room temperature to 700 °C in a nitrogen atmosphere. All the samples analyzed weighed 10 mg each.

Samples with a 1 cm x 1 cm were cut and placed inside the Thermo Nicolet Nexus™ 470 FT-IRESP Fourier Transform Infrared (FTIR) machine. The background spectrum was removed, then the samples were scanned in range of 400–4000 cm^{-1} with a resolution of 4 cm^{-1}.

2.7 Water Absorption

The water absorption test was conducted by weighing each dry sample and separately soaking them in DI water for three hours at room temperature. After removal, excess water was wiped off using filter paper and samples weighed. The water absorbed (%) by the composite NFs was determine by using the following formula:

$$Water\ Absorbed\ (\%) = \frac{W_f - W_i}{W_i}\ x\ 100$$

where W_f is the weight of the sample after it was submerged in water and W_i represents the dry sample weight. Three samples were used to replicate each condition and the average was reported.

2.8 Antibacterial Analysis

To test and examine the antibacterial properties of the fibers, the disk diffusion method was performed. All composite fiber samples were tested against gram-negative *Escherichia coli* (*E. coli*), a bacterium typically found in wounds. Each sample was cut using a coring tool with a 1 cm diameter to obtain a disk shape. Then, 25 mL of sterilized agar was poured into individual sterilized plates, followed by the introduction of the bacteria. The bacteria were then spread evenly throughout, and the disk-shaped samples were placed onto agar plates using two replicates per sample. Subsequently, the plates were placed in an incubator at 37 °C for 24 hours.

2.9 Cell Culture

NIH 3T3 mouse embryonic fibroblast cells were chosen to study cell adhesion and behavior. The cells were cultured in Dulbecco's Modified Eagle's Medium (DMEM), supplemented with 10% fetal bovine serum (FBS), 100 international units/milliliter ($IUmL^{-1}$) of penicillin, and 100μgmL^{-1} of streptomycin. Cells were maintained at 37 °C in a humidified incubator with 5% CO_2.

2.10 In Vitro Cell Process

For *in vitro* cell adhesion and proliferation studies, the composite NF membranes were cut at approximately 7 mm x 7 mm and placed in a 6-well cell culture plate. The samples were then sterilized under ultraviolet (UV) light for 10 minutes. In order to evaluate cell proliferation, 120,000 NIH 3T3 cells were seeded per sample in a 3-trail experiment, and incubated for 2, 4, and 6 days. After incubation, samples were first treated with Mito Tracker Red (MTR) for 20 minutes

followed by media and phosphate buffer saline (1XPBS) washes to remove non-adherent cells. Next, they were fixed with 4% formaldehyde for 30 minutes and stained with 300 nm 4′,6-diamino-2-phenylindole (DAPI) for 5 minutes. Afterward, membranes were washed twice with 1xPBS and mounted with 50% glycerol in order to be viewed using an Olympus® FV10i confocal laser scanning microscope.

3. Results and Discussions

3.1 Fiber Morphology Analysis

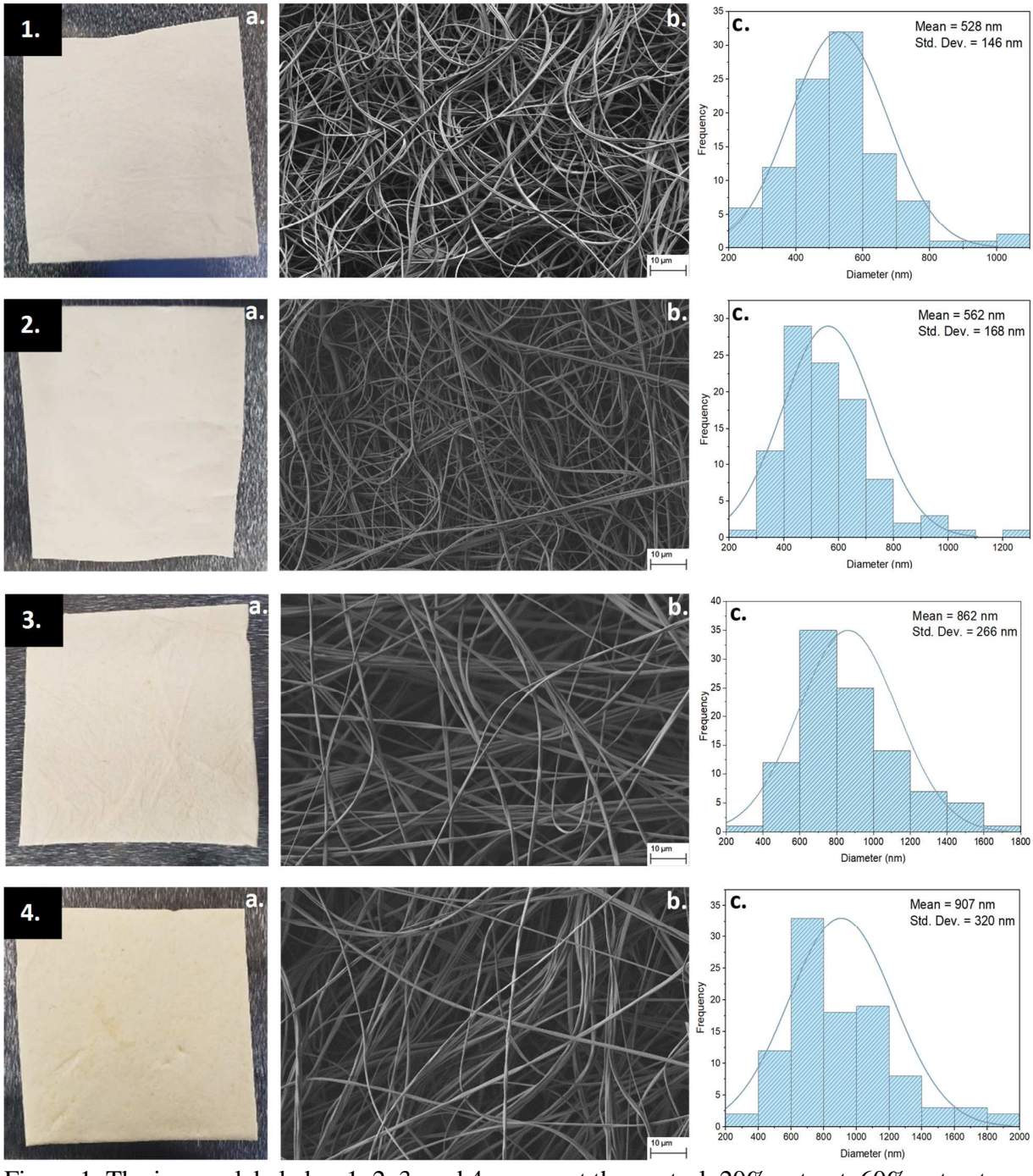

Figure 1. The images labeled as 1, 2, 3, and 4 represent the control, 20% extract, 60% extract, and 100% extract, respectively. Photographs of the cross-linked composite NF membranes (a),

scanning electron microscope (SEM) micrographs (b), and fiber diameter distributions (c). Scale bar = 10 μm.

Forcespinning® technology was chosen due to its high yield of NFs, combined with the wide variety of materials from which it can produce NFs. An optimization analysis of the composite NFs was performed and optimum parameters were found to be 5500-6500 rpm in a humidity of 45%-55%. Digital images of the developed membranes, SEM micrographs, and fiber diameter statistical analysis of the developed samples are shown in Figure 1 as a, b, and c, respectively. The obtained NFs exhibited long, smooth, and continuous fiber morphology as illustrated in Figure 1(b). The control sample had the lowest mean fiber diameter of 528 nm and a standard deviation of 146 nm, while samples prepared with 100% extract specimen showed the highest mean fiber diameter of 906.9 nm and a standard deviation of 320 nm. The data showed a positive correlation between the mean fiber diameter and the increase in AVE (Figure 1(c)). As is, the control sample is soluble in water, and therefore renders difficulties for use in wound dressing applications. CA was added to the system to crosslink polymeric molecules and enhance stability in aqueous media, effectively making them insoluble in water. These cross-linked membranes were submerged in water, removed, and analyzed under SEM, as shown in Figure 2.

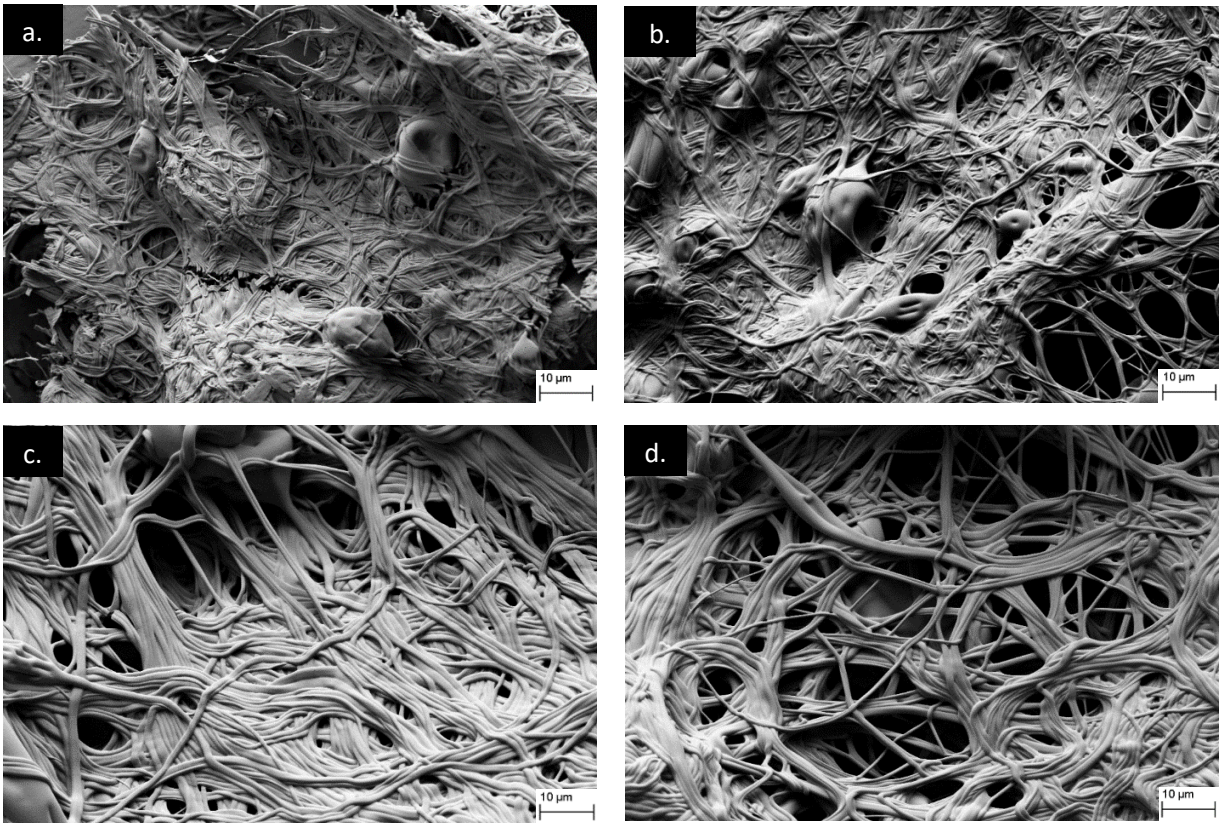

Figure 2. Image of cross-linked samples, control (a), 20% extract (b), 60% extract (c), and 100% extract (d), after being submerged in water.

3.2 Thermo-physical characterization

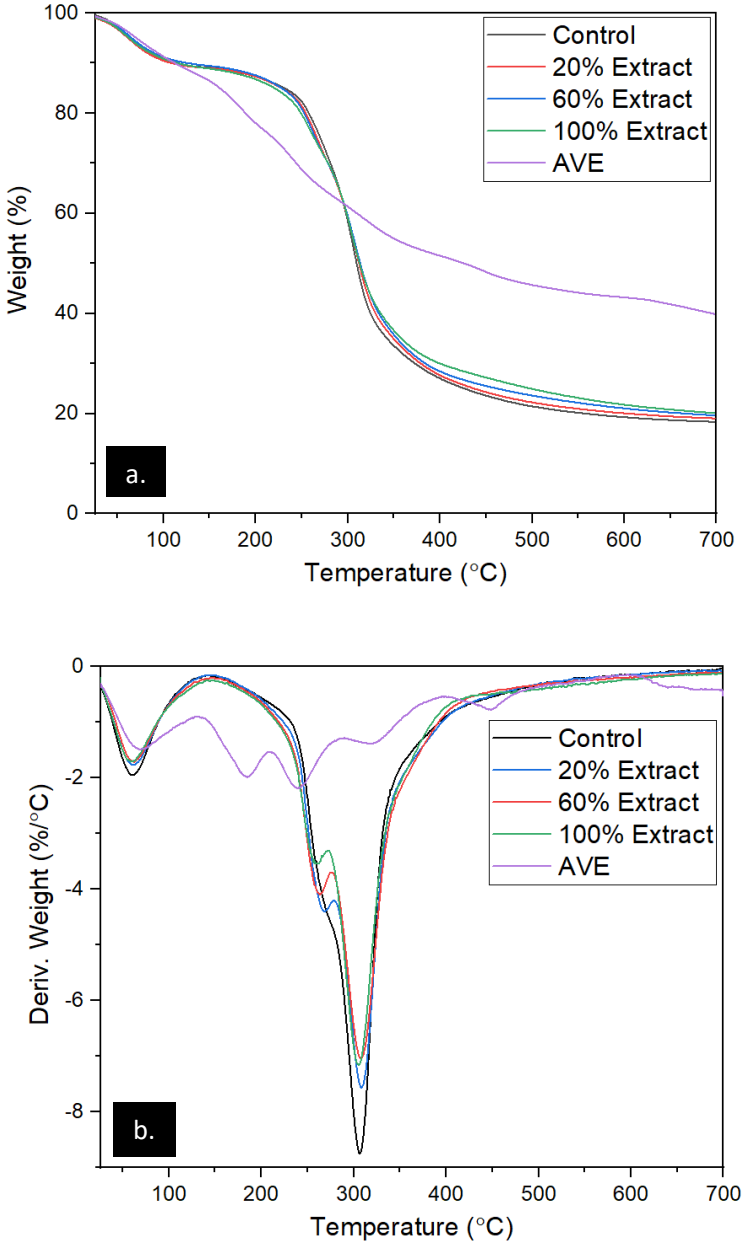

Figure 3. (a) TGA and (b) DTG analysis of the cross-linked composite NF membranes and lyophilized AVE.

Different thermogravimetric measurements were performed to analyze the thermal stability and the effect of *AVE* in the cross-linked composite NF membranes. The TGA and DTGA thermograms of the samples are shown in Figures 3. The lyophilized *AVE* followed multiple

degradation steps, starting with the loss of water content. Then the degradation process began and a weight loss at 210 °C to 290 °C was observed attributed to hemicellulose decomposition. Decomposition of cellulose and lignin were observed between from 300 to 395 °C and 400 to 520 °C, respectively. After 520 °C the weight loss was minimal due to the presence of fixed carbon [29, 30].

All the extract composite NF membranes show weight loss over two stages. The first one due to water loss. The second stage was the thermal degradation of the polymers starting at 150 °C. During this stage decomposition of the material began by the partial breaking of the molecular structure and disintegration of intermolecular bonds [31]. As the AVE content increased, the NF membranes exhibited a lower decomposition onset temperature (T_o), attributed to the initial thermal degradation of the AVE. Solaberrieta *et al.* obtained similar results; a decrease of the onset temperature decomposition with increasing AVE content in the polyethylene oxide (PEO) NF formulations [32]. Furthermore, the addition of AVE resulted in a small decrease in the maximum rate of thermal degradation temperature (Tmax). Even though the addition of AVE caused small changes in the T_o and the Tmax, it didn't affect the overall decomposition of the samples. A residual mass of 18.3%, 19%, 19.6%, and 20.1% for the control, 20%, 60%, and 100% extract, respectively, reflected the higher amount of AVE in the system.

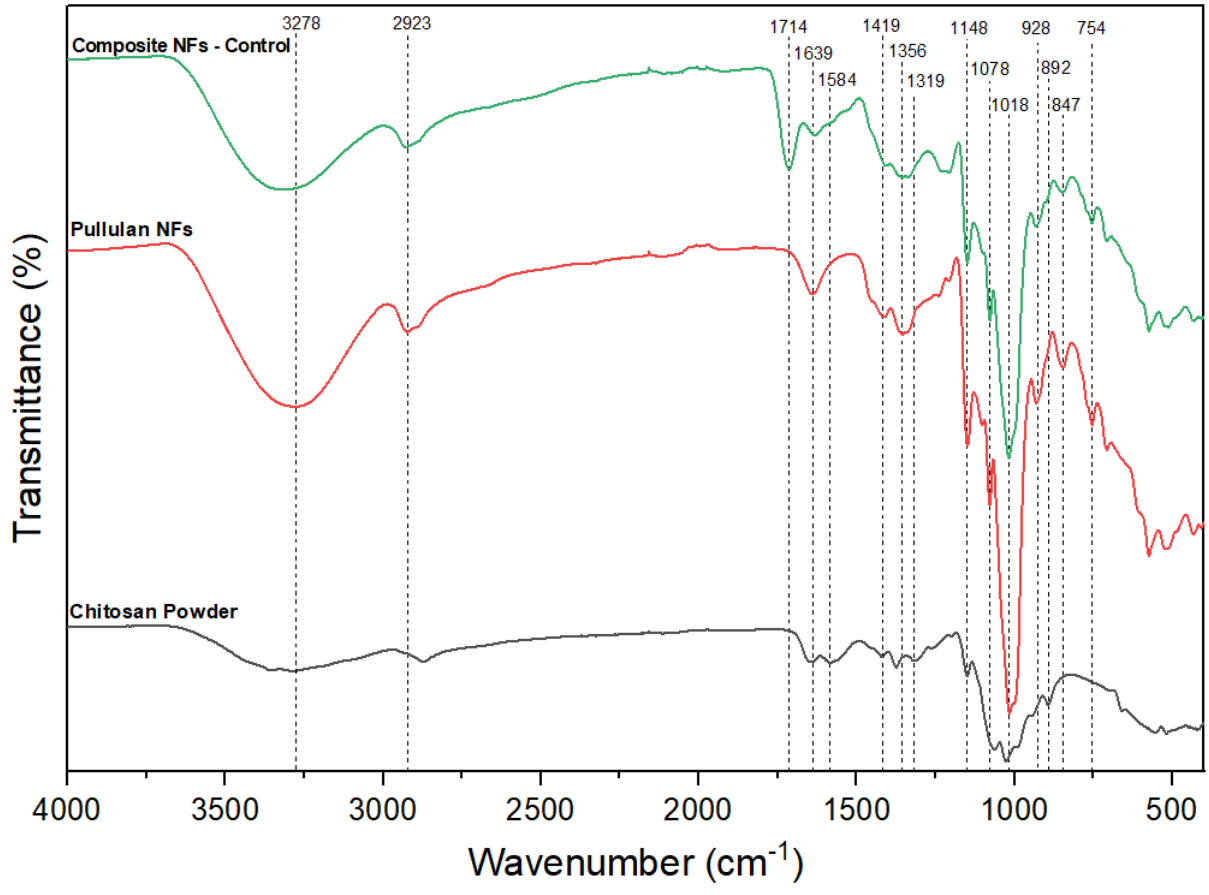

Figure 4. Fourier transform infrared (FTIR) spectrum of the composite NFs membrane control sample, pullulan NFs, and chitosan powder with characteristics bands.

The FTIR analysis was used to assess the functional groups present in the individual components, as well as the composite NF membranes. Figure 4 shows the spectra for the chitosan powder, pullulan NFs, and composite NFs. For pullulan, the broad band in the region around 3278 cm^{-1} was attributed to the O-H stretching and hydrogen bond originating from water molecules. The band at 2923 cm^{-1} corresponded to the C–H stretching [33]. A single band at 1,639 cm^{-1} was attributed to the stretching vibration of O–C–O. Other features were also observed in the spectra including C-O (1018 cm^{-1}), C–O–C stretch (1,148 cm^{-1}), and C–O–H bend (1,356 cm^{-1}), as reported by Singh and Saini [34]. An intense characteristic band of pullulan was located at 1078 cm^{-1}, which was due to the large proportion of the primary C-OH groups at the C-6 position. This

band was absent in the spectra for the chitosan, but it remained at 1078 cm^{-1} on the composite NF membrane, indicating that the added components did not affect the vibrational behavior for the C–OH group [35, 36].

In the chitosan spectra, a broad band at 3288 cm^{-1} corresponds to the O-H and N-H stretching [37]. The absorption band at around 2870 cm^{-1} is ascribed to the asymmetric C-H stretching, which is typical of polysaccharides. The bands at 1645 cm^{-1} (C=O stretching of amide I) and 1319 cm^{-1} (C-N stretching of amide III) confirmed the presence of residual N-acetyl groups. Characteristic absorption bands at 1584 cm^{-1}, 1419 cm^{-1} and 1374 cm^{-1} corresponded to the NH_2 bending of the primary amine, CH_2 bending, and the distorting vibration of C-CH_3, respectively [38, 39]. Additionally, the band at 1149 cm^{-1} can be attributed to C–O–C stretching vibration in the glucopyranose ring, and the absorption band at 895 cm^{-1} corresponds to the β(1 → 4) glycoside bridge structure [40].

The composite NF membrane shows a new band at 1714 cm^{-1}, which is attributed to the C=O stretching vibration due to the carbonyl group in CA. The absorption band at 847 cm^{-1} in the pullulan NFs is attributed to the α-configuration of α-D-glucopyranose units which decreased as a result of the addition of CS which contains β-glycosidic bonds [41]. Furthermore, bands found in the pullulan NFs spectra appeared in the composite NFs, including the bands at 754 cm^{-1} and 928 cm^{-1}, which prove the presence of pullulan's two main linkages: α-(1,4) glucosidic bonds and α-(1,6) glucosidic bands, respectively [42].

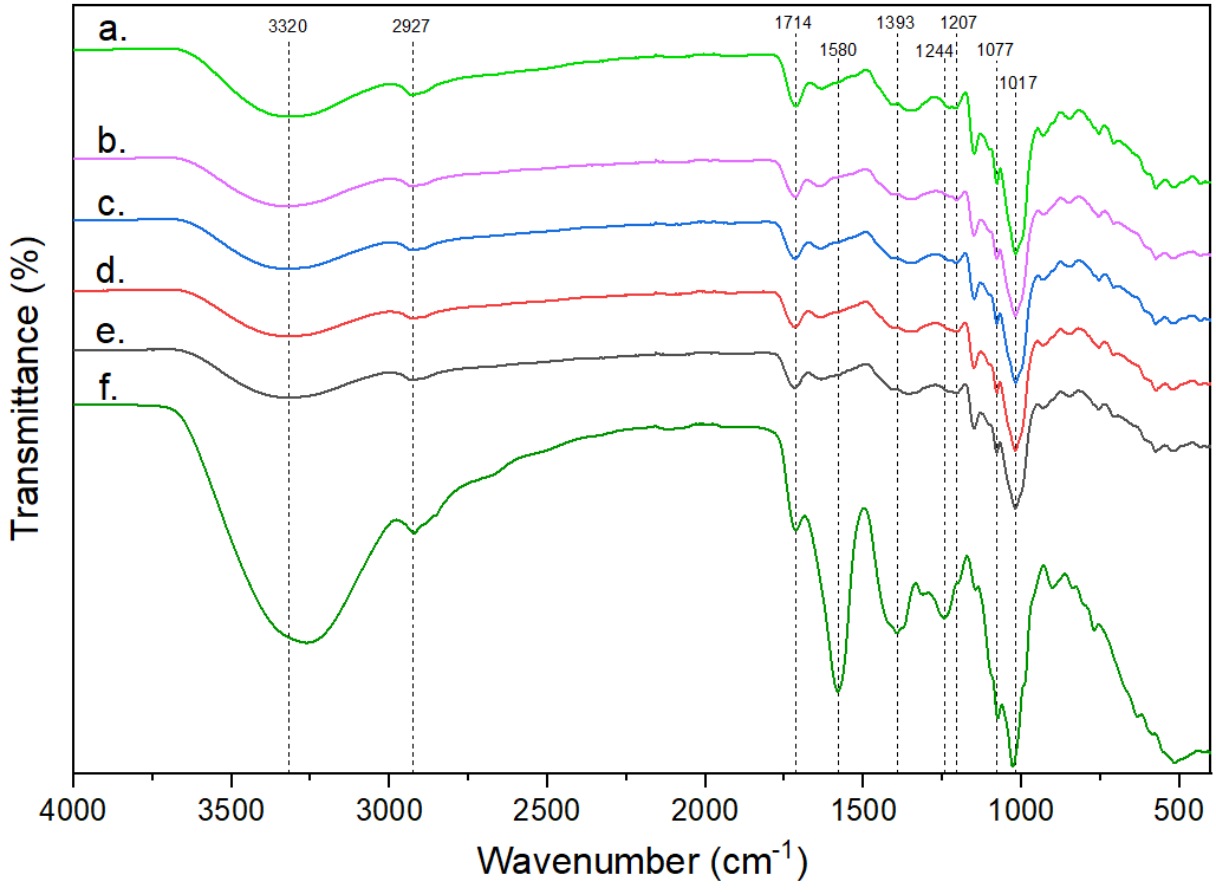

Figure 5. Fourier transform infrared (FTIR) spectrum of composite NFs membrane (a), cross-linked composite NFs membrane(b), cross linked composite NFs membrane with 20% extract (c), cross-linked composite NFs membrane with 60% extract (d), cross-linked composite NFs membrane with 100% extract (e), and lyophilized AVE (f).

The *A. vera* spectrum shown in Figure 5 illustrates a peak at 2927 cm^{-1} associated to the symmetrical and asymmetrical C–H stretching of the $-CH_2$ groups, indicating the presence of aliphatic (–CH) groups in these compounds. Absorption at 1714 cm^{-1} indicates a carbonyl peak (C=O) belonging to acids, ketones, and aldehydes [43]. The absorption bands at 1580 cm^{-1} and 1393 cm^{-1} are attributed to the C=C stretching and the symmetrical –COO stretching of carboxylate compounds in *A. vera*, respectively. Stretching vibrations of C–O groups of esters and phenols are attributed to the absorption at 1244 cm^{-1} [44, 45]. Furthermore, the shoulder peak at 1077 cm^{-1} is related to the C–O stretching associated with rhamnogalacturonan, and the high

intense band at 1017 cm^{-1} corresponds to the C–O and C–OH bonds of the glucan units in polysaccharides [46].

It was noted that an increase in the AVE content used to prepare the composite NF membranes reflected a subtly higher absorption band at 1580 cm^{-1}. The peak around 1600 cm^{-1} demonstrate the inclusion of *A. vera* [32]. After cross-linking, the band at 1207 cm^{-1} was slightly enhanced as a result of the etherification reaction between the hydroxyl and carbonyl groups of pullulan and CA [47]. The combination of pullulan, CA, CS, and *A. vera* did not have any substantial changes in the chemical composition, which allowed them to maintain their individual properties. As a result, the thermal stability, antibacterial, and biological potential effects were maintained.

3.3 Water Absorption

The water absorption capability of composite NF membranes was measured to be 495 ± 20%, 388 ± 23%, 430 ± 21%, and 310 ± 26% for the control, 20% ex, 60% ex, and 100% ex, respectively. It can be observed that water absorption of the samples with AVE was lower than the control. AVE inhibits water molecule diffusion into the fibers, resulting in a lower absorption [48]. However, all the samples still exhibit high absorptivity due to the NFs high surface-area-to-volume ratio. This is a desirable characteristic in wound dressings to help in the removal of exudates, especially in highly exudating wounds, in addition to creating a favorable environment for cell adhesion and growth [49, 50]. The produced membranes demonstrated the absorption needed for optimal wound dressing while maintaining adequate structure stability.

3.4 Fiber Antibacterial Results

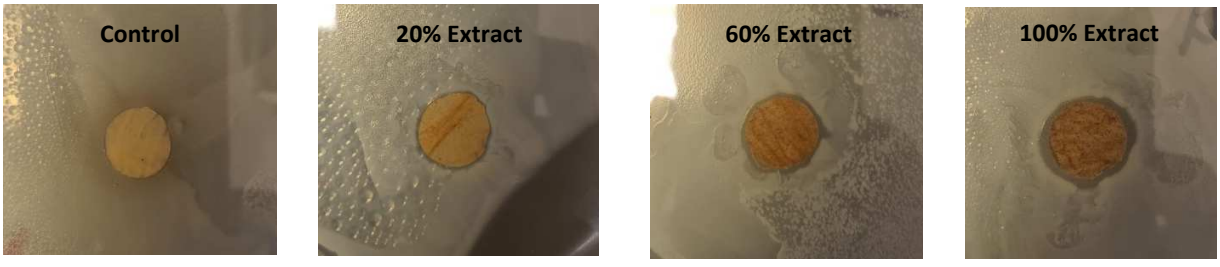

Figure 6. Image of cross-linked nonwoven composite NFs tested against *E. coli*.

Figure 6 shows the results for the control and *A. vera* based containing nanofiber mats exposed to *E. coli* bacteria. As it can be observed, the control samples showed no zone of inhibition against the bacteria, while mats containing A. vera depict clear inhibition zones, indicating antibacterial activity. The samples containing 20%, 60% and 100% AVE resulted in inhibition zones of 1 mm, 2 mm, and 2.5 mm, respectively. These results illustrate that the antibacterial properties of the nonwoven composite NFs were enhanced as the concentration of AVE increased.

A. vera is used in skin related treatments due to its antifungal, anti-inflammatory, antiviral, and antibacterial activity against multiple types of infections. In a previous study, *A. vera* antibacterial properties against gram-negative *E. coli* and other bacteria have also demonstrated effective antimicrobial efficacy [51]. The mechanism by which *A. vera* exerts its antibacterial action is believed to be associated to anthraquinones. Anthraquinones act as tetracycline, which blocks the ribosomal A site, thus, inhibiting the bacterial protein synthesis and preventing the bacteria from growing [52]. Furthermore, *A. vera* possess a hydroxylated phenol known as pyrocatechol, which is proven to be toxic to micro-organisms. The number of present hydroxyl groups on the phenol group is correlated to the level of micro-organism toxicity (i.e. the more hydroxyl groups present, the more toxic to micro-organisms). These phenolic groups are responsible for the cell membrane disruption, as well as the denaturing of bacterial cell protein.

Additionally, other studies have reported the ascorbic acid found in Aloe vera, acts as a strong antibacterial agent that inhibits enzymatic activity and interferes with bacterial cell membrane and genetic mechanisms [53]. The amount of active biological components present in the samples are essential for the antibacterial activity as observed in the results obtained.

3.5 Fiber *In Vitro* Cell Adhesion and Proliferation

Cell adhesion and proliferation were analyzed on the composite NF membranes after 2, 4, and 6 days (shown in Figure 7). Samples were analyzed using DAPI staining, a technique which is used to determine cells viability by identifying its nuclear morphology in colocalization assays [54]. MitoTracker Red CMXRos is a cell-permeable red fluorescent dye that accumulates in the negatively charged mitochondrial matrix and allows for detection of the mitochondrial membrane potential. The mitochondrial membrane potential is a key indicator of cell health; healthy cells accumulate more dye compared to apoptotic cells [55]. It was observed that MitoTracker was present in all samples, indicating that the cells were viable within a nanofibrous membrane, with the exception of day 4 of incubation in the 60% extract sample. Additionally, cells showed MitoTracker signal in the following days, which demonstrated that the cells maintained their initial health. MitoTracker further revealed the mitochondrial network within cells, providing a marker of cellular morphology within the nanofibrous structure of AVE NF composites. Furthermore, cell nuclei are clearly apparent in all samples, with a constant number of cells appearing each day. There was a high number of cells on day 6 for the 60% extract sample and the presence of clusters within some of the other NF composites. Cells display a multipolar morphology with cellular extensions with an increase of AVE, as compared to the rounded cell morphology present in control samples. These observations may be due to the water absorption capabilities conferred by

A. vera, enabling further interactions between the fibrous structure and cells due to the uptake and retention of the cell culture medium.

To quantify cell density, average cell count/image was calculated from 10 images per trial for each fiber type, and an ANOVA post-hoc Tukey statistical analysis was conducted (Figure 8). After a 2-day incubation period, no significant difference (P-value: 0.2587) was shown in the comparison of all samples. Day 4 displayed no significant difference (P-value: 0.0568) between all samples, while at day 6, all samples were shown to have no significant difference (P-value: 0.6703) to the control. While there is variability between the values found in each respective sample, as shown through the high standard error bars, each AVE-incorporating sample supported cell growth as demonstrated by confocal microscopy. The results demonstrate that AVE-incorporating fibers do not inhibit cell adhesion as compared with controls, allowing effective cell proliferation on these biocompatible nanofibrous membranes.

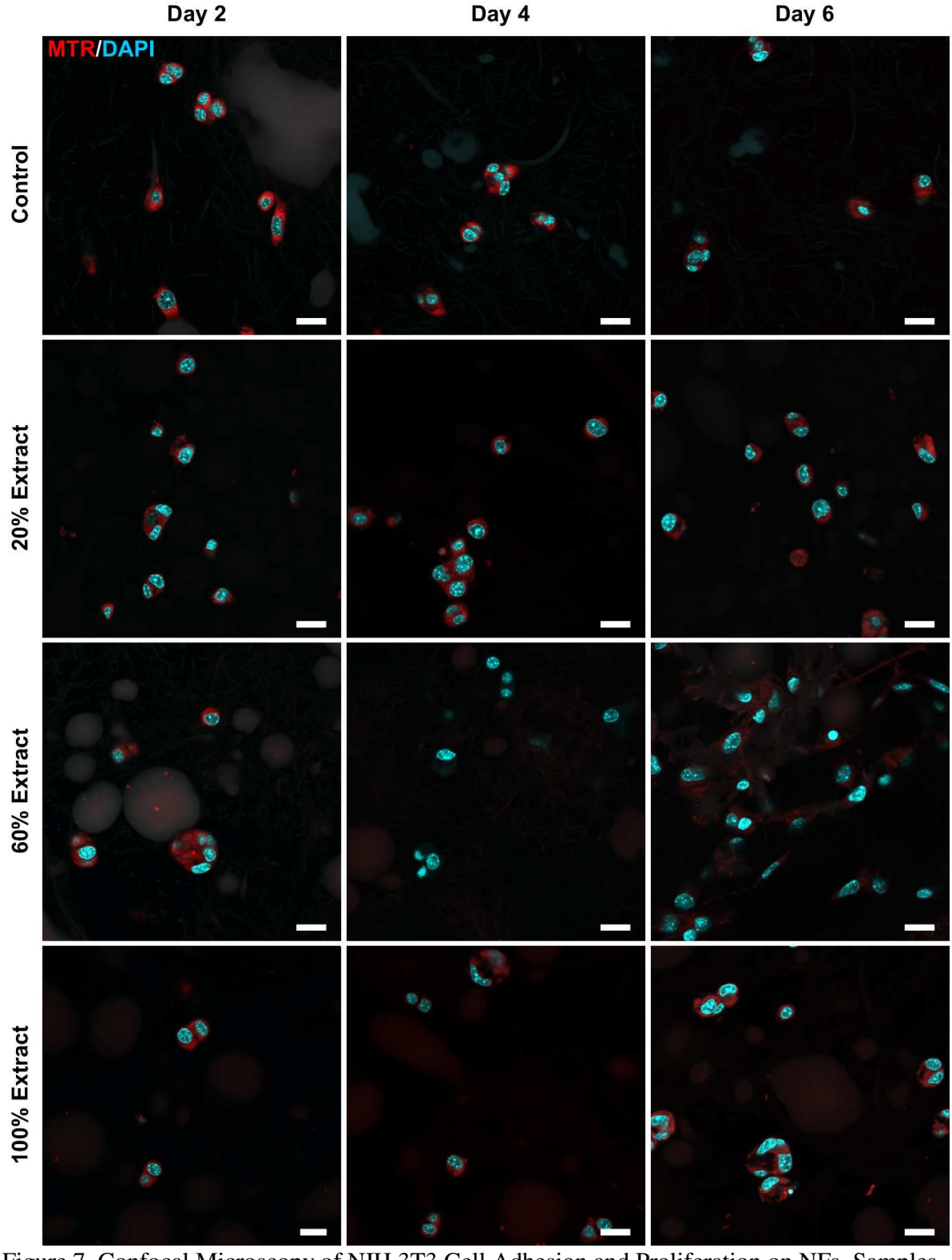

Figure 7. Confocal Microscopy of NIH 3T3 Cell Adhesion and Proliferation on NFs. Samples were treated with DAPI (blue) for the presence of the nucleus and MTR (red) for the presence of the mitochondria. n = 3 trial experiment. Image size 212 x 212 μm, with a scale bar = 20 μm.

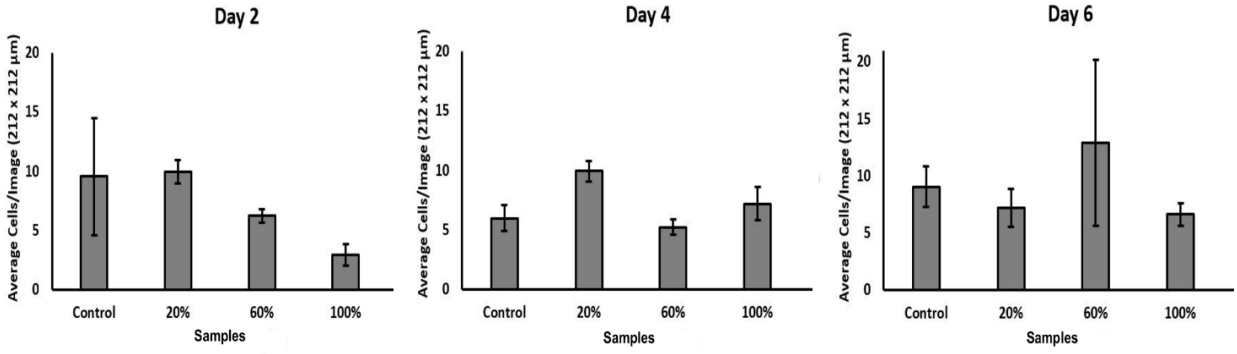

Figure 8. Cell proliferation results from a 3-trial experiment for cross-linked composite NF membrane samples: control, 20%, 60%, and 100% extract. An ANOVA post-hoc Tukey statistical analysis is shown ($P > 0.05$).

4. Conclusion

Biocompatible composite NFs with synergistic antibacterial activity against *E. coli* and capability to promote cell attachment and growth were successfully produced via Forcespinning® method. The NFs produced were made from natural biocompatible, biodegradable products which included *A. vera* extract, pullulan, chitosan, and citric acid. *In vitro* cell culture experiments illustrate that the developed antibacterial composite samples are non-cytotoxic to NIH 3T3 fibroblast cells and allow effective fibroblast cell attachment, as well as interlayer cell growth. Its porous and high surface area structure makes it a potential candidate for wound dressing application, absorbing excessive blood and exudates, as well as providing protection from infection while displaying good thermal stability. The methods employed here could be suitable to produce different biocompatible composite NFs from other materials to obtain similar physicochemical properties for wound dressing or a wide range of other applications.

CRediT author contribution statement

Raul Barbosa: Conceptualization, Methodology, Investigation, Validation, Writing - Original Draft. **Alexa Villareal:** Validation, Investigation, Data Curation. **Cristobal Rodriguez:** Validation, Investigation. **Heriberto de Leon:** Validation, Investigation. **Robert Gilkerson:** Validation and resources. **Karen Lozano:** Supervision, Resources, Writing - Review & Editing, and Funding acquisition.

Declaration of competing interest

The authors declare that they have no known competing financial interests or personal relationships that could have appeared to influence the work reported in this paper.

Acknowledgement

Authors gratefully acknowledge funding from National Science Foundation under PREM grant DMR 1523577.

Data availability

The raw/processed data required to reproduce these findings cannot be shared at this time as the data also forms part of an ongoing study.

References

[1] Orgill, Dennis P., and Carlos Blanco, eds. Biomaterials for treating skin loss. Elsevier, 2009.

[2] Guo, S. al, and Luisa A. DiPietro. "Factors affecting wound healing." Journal of dental research 89.3 (2010): 219-229.

[3] Järbrink, Krister, et al. "Prevalence and incidence of chronic wounds and related complications: a protocol for a systematic review." Systematic reviews 5.1 (2016): 152.

[4] Abrigo, Martina, Sally L. McArthur, and Peter Kingshott. "Electrospun nanofibers as dressings for chronic wound care: advances, challenges, and future prospects." Macromolecular bioscience 14.6 (2014): 772-792.

[5] “Classification: USDA PLANTS.” Classification | USDA PLANTS, plants.usda.gov/java/ClassificationServlet?source=profile.

[6] Maenthaisong, Ratree, et al. "The efficacy of aloe vera used for burn wound healing: a systematic review." burns 33.6 (2007): 713-718.

[7] Visuthikosol, V., et al. "Effect of aloe vera gel to healing of burn wound a clinical and histologic study." J Med Assoc Thai 78.8 (1995): 403-9.

[8] Syed, Tanweer A., et al. "Management of psoriasis with Aloe vera extract in a hydrophilic cream: a placebo-controlled, double-blind study." Tropical Medicine & International Health 1.4 (1996): 505-509.

[9] Fulton Jr, James E. "The stimulation of postdermabrasion wound healing with stabilized aloe vera gel-polyethylene oxide dressing." The Journal of dermatologic surgery and oncology 16.5 (1990): 460-467.

[10] Jithendra, Panneerselvam, et al. "Preparation and characterization of aloe vera blended collagen-chitosan composite scaffold for tissue engineering applications." ACS applied materials & interfaces 5.15 (2013): 7291-7298.

[11] Suganya, S., et al. "Aloe vera incorporated biomimetic nanofibrous scaffold: a regenerative approach for skin tissue engineering." Iranian Polymer Journal 23.3 (2014): 237-248.

[12] Ferro, Valerie A., et al. "In vitro susceptibilities of Shigella flexneri and Streptococcus pyogenes to inner gel of Aloe barbadensis Miller." Antimicrobial agents and chemotherapy 47.3 (2003): 1137-1139.

[13] Radha, Maharjan H., and Nampoothiri P. Laxmipriya. "Evaluation of biological properties and clinical effectiveness of Aloe vera: A systematic review." Journal of traditional and complementary medicine 5.1 (2015): 21-26.

[14] Zhang, Linna, and Ian R. Tizard. "Activation of a mouse macrophage cell line by acemannan: the major carbohydrate fraction from Aloe vera gel." Immunopharmacology 35.2 (1996): 119-128.

[15] Bradbury, Savile, and David C. Joy. “Scanning Electron Microscope.” Encyclopædia Britannica, Encyclopædia Britannica, Inc., 30 Oct. 2019, www.britannica.com/technology/scanning-electron-microscope.

[16] Ren, Yan, et al. "The preparation and structure analysis methods of natural polysaccharides of plants and fungi: A review of recent development." Molecules 24.17 (2019): 3122.

[17] Trinetta, V., and C. N. Cutter. "Pullulan: A suitable biopolymer for antimicrobial food packaging applications." Antimicrobial Food Packaging. Academic Press, 2016. 385-397.

[18] Abhilash, M., and D. Thomas. "Biopolymers for biocomposites and chemical sensor applications." Biopolymer Composites in Electronics. Elsevier, 2017. 405-435.

[19] Singh, Ram Sarup, Navpreet Kaur, and John F. Kennedy. "Pullulan and pullulan derivatives as promising biomolecules for drug and gene targeting." Carbohydrate Polymers 123 (2015): 190-207.

[20] Hasegawa, Urara, et al. "Nanogel-quantum dot hybrid nanoparticles for live cell imaging." Biochemical and biophysical research communications 331.4 (2005): 917-921.

[21] Popa, Valentin. Polysaccharides in medicinal and pharmaceutical applications. Smithers Rapra, 2011.

[22] Wong, Victor W., et al. "Engineered pullulan–collagen composite dermal hydrogels improve early cutaneous wound healing." Tissue engineering part A 17.5-6 (2011): 631-644.

[23] Li, Huanan, et al. "Superabsorbent polysaccharide hydrogels based on pullulan derivate as antibacterial release wound dressing." Journal of Biomedical Materials Research Part A 98.1 (2011): 31-39.

[24] Xu, Fenghua, et al. "Development of tannic acid/chitosan/pullulan composite nanofibers from aqueous solution for potential applications as wound dressing." Carbohydrate polymers 115 (2015): 16-24.

[25] Lozano, Karen, and Kamalaksha Sarkar. "Methods and apparatuses for making superfine fibers." U.S. Patent Application No. 12/404,907.]

[26] [Sarkar, Kamal, et al. "Electrospinning to forcespinning™." Materials today 13.11 (2010): 12-14.]

[27] [Padron, Simon, et al. "Experimental study of nanofiber production through forcespinning." Journal of applied physics 113.2 (2013): 024318.]

[28] Cremar, Lee, et al. "Development of antimicrobial chitosan based nanofiber dressings for wound healing applications." Nanomedicine Journal 5.1 (2018): 6-14.

[29] Hanafiah, Megat Ahmad Kamal Megat, et al. "Methylene blue adsorption on Aloe vera rind powder: Kinetics, Isotherm and Mechanisms." Nature Environment and Pollution Technology 17.4 (2018): 1055-1064.

[30] Pathak, Pranav D., Sachin A. Mandavgane, and Bhaskar D. Kulkarni. "Characterizing fruit and vegetable peels as bioadsorbents." Current Science (2016): 2114-2123.

[31] Lewandowska, Katarzyna. "Miscibility and thermal stability of poly (vinyl alcohol)/chitosan mixtures." Thermochimica Acta 493.1-2 (2009): 42-48.

[32] Solaberrieta, Ignacio, et al. "Encapsulation of Bioactive Compounds from Aloe Vera Agrowastes in Electrospun Poly (Ethylene Oxide) Nanofibers." Polymers 12.6 (2020): 1323.

[33] Wu, Jia, et al. "Preparation and characterization of pullulan–chitosan and pullulan–carboxymethyl chitosan blended films." Food Hydrocolloids 30.1 (2013): 82-91.

[34] Singh, R. S., and G. K. Saini. "Pullulan-hyperproducing color variant strain of Aureobasidium pullulans FB-1 newly isolated from phylloplane of Ficus sp." Bioresource technology 99.9 (2008): 3896-3899.

[35] Tong, Qunyi, Qian Xiao, and Loong-Tak Lim. "Preparation and properties of pullulan–alginate–carboxymethylcellulose blend films." Food Research International 41.10 (2008): 1007-1014.

[36] Shingel, Kirill I. "Determination of structural peculiarities of dexran, pullulan and γ-irradiated pullulan by Fourier-transform IR spectroscopy." Carbohydrate Research 337.16 (2002): 1445-1451.

[37] Xu, Y. X., et al. "Chitosan–starch composite film: preparation and characterization." Industrial crops and Products 21.2 (2005): 185-192.

[38] Fernandes Queiroz, Moacir, et al. "Does the use of chitosan contribute to oxalate kidney stone formation?." Marine drugs 13.1 (2015): 141-158.

[39] Wang, Qun, et al. "Controlled release of ciprofloxacin hydrochloride from chitosan/polyethylene glycol blend films." Carbohydrate polymers 69.2 (2007): 336-343.

[40] He, Guanghua, et al. "Synthesis, characterization and antibacterial activity of salicyloyl chitosan." Carbohydrate polymers 83.3 (2011): 1274-1278.

[41] Shi, Rui, et al. "The effect of citric acid on the structural properties and cytotoxicity of the polyvinyl alcohol/starch films when molding at high temperature." Carbohydrate polymers 74.4 (2008): 763-770.

[42] Cheng, Kuan-Chen, Ali Demirci, and Jeffrey M. Catchmark. "Effects of plastic composite support and pH profiles on pullulan production in a biofilm reactor." Applied microbiology and biotechnology 86.3 (2010): 853-861.

[43] Abbasi, Muhammad SA, Muhammad Aslam Tahir, and Sidra Meer. "FTIR Spectroscopic study of aloe vera barbadensis Mill Buds." Asian Journal of Chemical Sciences (2020): 1-6.

[44] Lim, Zhe Xi, and Kuan Yew Cheong. "Effects of drying temperature and ethanol concentration on bipolar switching characteristics of natural Aloe vera-based memory devices." Physical Chemistry Chemical Physics 17.40 (2015): 26833-26853.

[45] Jithendra, Panneerselvam, et al. "Preparation and characterization of aloe vera blended collagen-chitosan composite scaffold for tissue engineering applications." ACS applied materials & interfaces 5.15 (2013): 7291-7298.

[46] Torres-Giner, Sergio, et al. "Nanoencapsulation of Aloe vera in synthetic and naturally occurring polymers by electrohydrodynamic processing of interest in food technology and bioactive packaging." Journal of Agricultural and Food Chemistry 65.22 (2017): 4439-4448.

[47] Li, Zongjie, et al. "Preparation and characterization of long-term stable pullulan nanofibers via in situ cross-linking electrospinning." Adsorption Science & Technology 37.5-6 (2019): 401-411.

[48] Sirima, Sutasinee, Manisara Phiriyawirut, and Khomson Suttisintong. "Comparison of the Release of Aloe vera Extracts from Poly (Vinyl Alcohol) Electrospun Fibers and Hydrogel Films for Wound Healing Applications." Key Engineering Materials. Vol. 751. Trans Tech Publications Ltd, 2017.

[49] Lalani, Reza, and Lingyun Liu. "Electrospun zwitterionic poly (sulfobetaine methacrylate) for nonadherent, superabsorbent, and antimicrobial wound dressing applications." Biomacromolecules 13.6 (2012): 1853-1863.

[50] Skórkowska-Telichowska, Katarzyna, et al. "The local treatment and available dressings designed for chronic wounds." Journal of the American Academy of Dermatology 68.4 (2013): e117-e126.

[51] Athiban, Prakash P., et al. "Evaluation of antimicrobial efficacy of Aloe vera and its effectiveness in decontaminating gutta percha cones." Journal of conservative dentistry: JCD 15.3 (2012): 246.

[52] Pandey, Ruchi, and Avinash Mishra. "Antibacterial activities of crude extract of Aloe barbadensis to clinically isolated bacterial pathogens." Applied biochemistry and biotechnology 160.5 (2010): 1356-1361.

[53] Lawrence, Rubina, Priyanka Tripathi, and Ebenezer Jeyakumar. "Isolation, purification and evaluation of antibacterial agents from Aloe vera." Brazilian Journal of Microbiology 40.4 (2009): 906-915.

[54] Geisler, Sven, et al. "PINK1/Parkin-mediated mitophagy is dependent on VDAC1 and p62/SQSTM1." Nature cell biology 12.2 (2010): 119-131.

[55] Perry, Seth W., et al. "Mitochondrial membrane potential probes and the proton gradient: a practical usage guide." Biotechniques 50.2 (2011): 98-115.

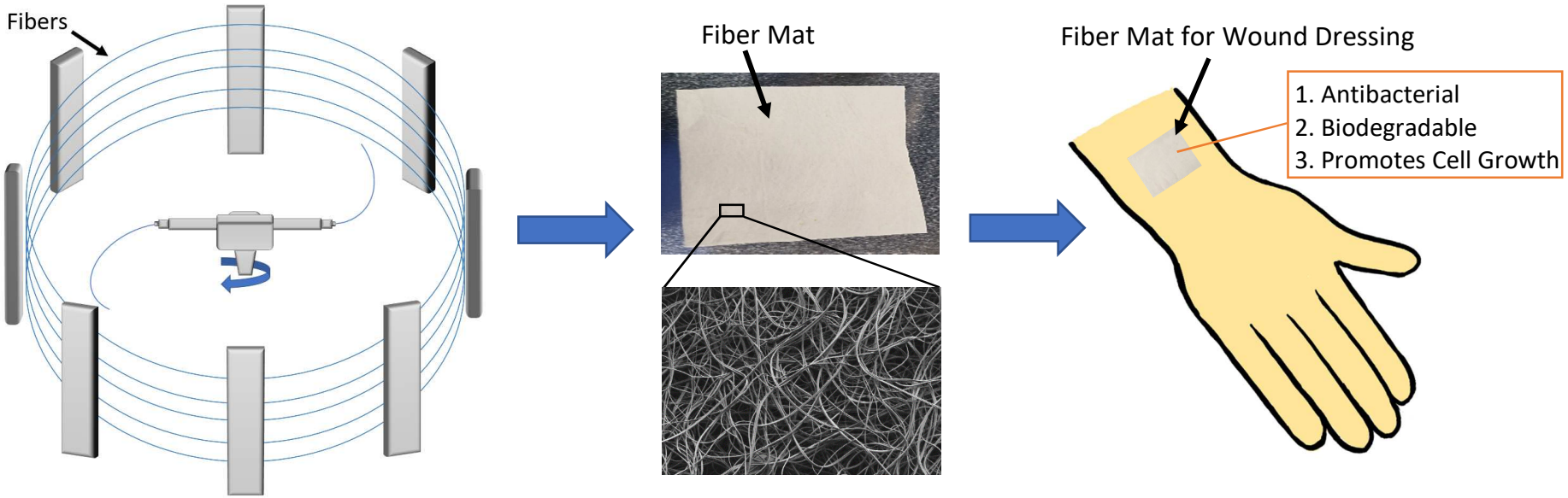
Fibers
Fiber Mat
Fiber Mat for Wound Dressing
1. Antibacterial
2. Biodegradable
3. Promotes Cell Growth